American Scientific Research Journal for Engineering, Technology, and Sciences (ASRJETS)
ISSN (Print) 2313-4410, ISSN (Online) 2313-4402

http://asrjetsjournal.org/

Girder Load Share for the Curved I-Girder Bridge Subjected to the Point Load

Amer Izzet[a*], Aymen Mohammed[b]

[a]*University of Baghdad/College of Engineer/Civil Engineering Dept., Assistant Prof. , Iraq.*
[b]*University of Baghdad/College of Engineer/Civil Engineering Dept. PhD Student. , Iraq.*
[a]*Email: amer.f@coeng.uobaghdad.edu.iq, amerfarouk@yahoo.com*
[b]*Email: aymenrm@yahoo.com*

Abstract

The objective of this research is to study experimentally and theoretically the girder vertical load share of the curved I-Girder bridges subjected to the point load in addition to the self-weigh and supper imposed dead loads. The experimental program consist of manufacturing and testing the five simply supported bridge models was scaled down by (1/10) from a prototype of 30m central span. The models carriageway central radii are 30 m, 15m or 10m. The girder spacing of the first two models is 175 mm with an overall carriageway width of 650mm. The girder spacing of the other three bridge models is 200mm with the overall carriageway width of 700 mm. The overall depth of the composite section was 164 mm. To investigate the effect of live load position on the girder vertical load share a point load was applied at different load levels and was varied across bridge width. Experimental results show that the main factor effect on the girder load share were the point load position, load level and the bridge curvature value, while the girder spacing had a less effect than that. The ANSYS Worckbench 14.5 commercial software was adopted to build up the Finite Element model. Results have shown that the numerical model was slightly stiffer than the experimental test bridge model. A good agreement was obtained between the experimental and analytical results for all models, the maximum deviation in results reach to13% in such a single case, while the convergence results are the prevailing situation.

Keywords: Curved I-Girder; Point Load; Girder Load share; Curvature; girder spacing.

---

* Corresponding author.

1. Introduction

The additional moment generated on system due to curvature causes some girder in curved bridge deck carry a vertical load greater than the adjacent girder as shown in the Figure 1. Barré de Saint Venant was the first one presented the analysis of curved beams in 1843 as referred by [2]. Allowable Stress Design (ASD) or Working Stress Design (WSD) was being a result of joint efforts of Consortium of University Research Teams (CURT) with the tam of University of Maryland. Load Factor Design (LFD) criteria adopted by AASHTO 1993 [3], to go along with the ASD criteria and appeared in the first Guide in1980 as well as the Guide of1993 [4]. The National Cooperative Highway Research Program (NCHRP) was developed a set of improved specifications in 1993, this project was aimed at improving the LFD. American Iron and Steel Institute (AISI) and FHWA in 1999 extend the results of experimental tests conducted under the CURT project and Curved Steel Bridge Research Project (CSBRP) was initiated by FHWA in 1992. Because of the difficulty and complexity in the solution of the differential equation governing the behavior of curved I-Girder system, alternative analysis methods may be adopt and considered as easier and sufficiently accurate methods, there for the girder vertical load share as a stress ratio represent the mid-span girder longitudinal stresses to the bridge deck sectional stress response will be investigated in this research under point load, Figure1 shows the effect of the lateral bending moment on the vertical load share in curved I-girder bridges.

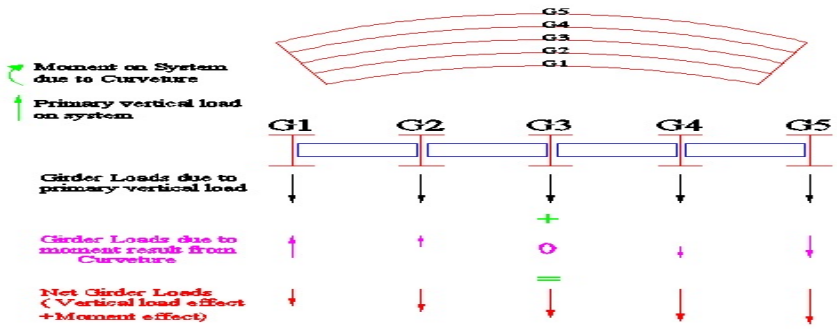

Figure 1: Vertical load share in curved I-girder bridges

2. Material and Methods

2.1. Experimental Work

1. Material and manufacturing of the bridge models

Cold bending process was adapted to forming the curvature for the IPN 120 steel rolled section [5]. The tensile properties before and after cold bending were investigated by testing a coupons cut from flanges and webs for three curvatures values 0.10, 0.20 and 0.3 radians are shown in Table1. The maximum deviation percent between the yield and ultimate stresses before and after cold bending reached to 7.1% and 5.8% respectively. On the other hand, two types of plate (3.50 mm thick) coupons were tested; the first without welding and the other welded along its one edge, the yield tensile strength was 355 MPa and 418.9 MPa respectively with deviation percent was 18%, So, the used of cold bending to forming the curvature of the steel rolled section is better than that of using welding to built-up section from steel plate (small thickness Plate) in case of model

fabrication. The average deck concrete compressive strength was 35.19 MPa. The tensile properties of slab reinforcement (3.85 mm in diameter) gave a yield strength of 650 MPa and ultimate strength of 815.6 MPa. The central span, radius of curvature, girder spacing is shown in Table 2. The Figure 2 shows the typical section of the bridge model and the Figure 3 shows the elements of the bridge model section. In order to simulate the prototype girder section, a reducing of the top flange width symmetrically for both sides from (64mm) to (50mm). Steel plate of 2 mm thickness was used to modeling the diaphragms and transverse stiffeners, the assemblage of model components (girders, diaphragms, stiffeners and shear connectors) was conducted by welding model parts together using low temperature system to reduce the welding deformations, Fixing the wood formwork and assembly the double layer bars of 3.85mm diameter for deck reinforcement as show in the Figure 4.

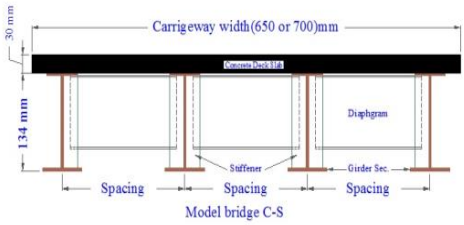

Figure 2: Typical section of the

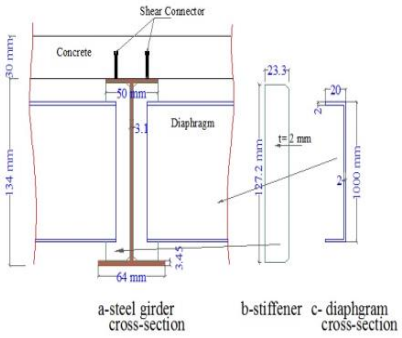

Figure 3: Typical Bridge

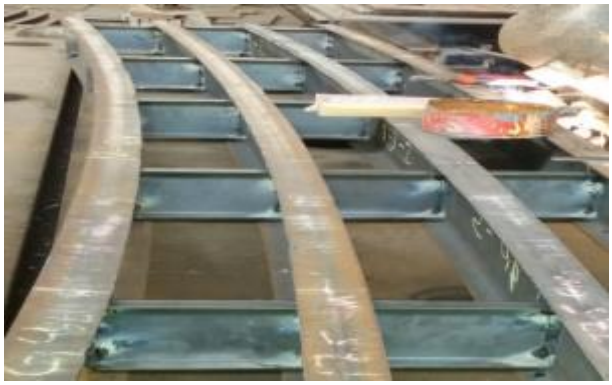

a- Welding Diaphragms with steel curve girders

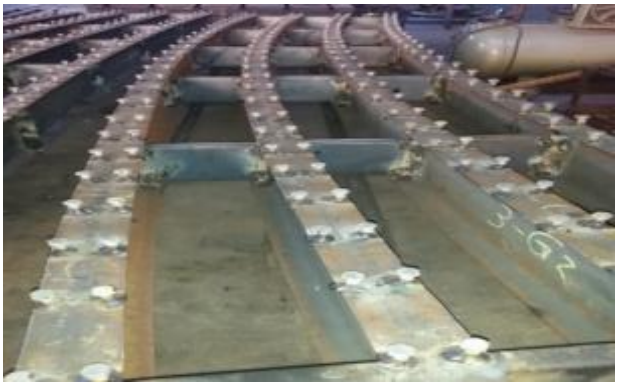

b- Welding the shear connector.

c- Wooden formwork of reinforced concrete deck slab

d- Casting the concrete of deck slab

Figure 4: Assemblage of the bridge model components.

Table 1: Mechanical properties of the bridge model components.

Properties	L/R=0.10			L/R=0.20			L/R=0.30		
	FC	WC	DC	FC	WC	DC	FC	WC	DC
Thickness (mm)	3.45	3.10	1.96	3.45	3.10	1.96	3.45	3.10	1.96
Yield Stress bb(MPa)	352.7	351.03	355.31	352.7	351.03	355.31	352.7	351.03	355.31
Yield Stress ab (MPa)	364.86	359.80	-----	372.09	365.10	-----	377.76	371.46	-----
% of Deviation in Yield Stress	3.44	2.49	----	5.49	4.0	----	7.10	5.80	----
Ultimate stress bb (MPa)	499.6	492.96	453.6	499.6	492.96	453.6	499.6	492.96	453.6
Ultimate Stress ab (MPa)	514.58	508.28	----	523.48	517.15	----	529.6	521.57	----
% of Deviation in Ultimate Stress	3.0	3.1	----	4.78	4.90	----	5.70	5.80	----
Elongation bb%	14.60	13.91	17.16	14.60	13.91	17.16	14.60	13.91	17.16
Elongation % (ab)	14.75	14.50	----	14.90	15.20	----	15.20	15.60	----

Where; **bb** means before bending, **ab** means after bending, **FC** means flange coupon, **WC** means web coupon and **DC** means diaphragm coupon.

2. Instrumentation

Four FLA-6-11 strain gauges were used to measure the generated longitudinal strains in the lower surface of the bottom girder flanges at mid-span. Figure 5 shows the location of the strain gauges for the bridge model. The reading from these strain gauge recorded by a strain indicator connected to the personal computer. The application of point loads was by using a manual jack of 20 Tons, load cell of 30 Tons capacity, the top transverse IPN220 steel beam was fixing to the drop down shaft, therefor the pressure coming up from manual jack will reflect to the load cell and then to the bridge model. The loads for the stresses similitude under self-weight (SW), super imposed dead (SIDL) loads are called as an equivalent loads, these loads were calculated by idealizing both the full scale bridge and scale down bridge model by finite element method and performing the structural analysis to evaluate the maximum generated girder longitudinal bottom flange stresses, as shown in Table 3.

3. Test Procedure

This test was carried out to investigate the vertical load share of each girder due to point load moving transversely across the width of the bridge model, the equivalents Self-Weight (SW)and the equivalents superimposed (SIDL) were applied using sand bags and steel weights(shafts, rectangular prism and steel blocks) before applying the concentrated load increments. The concentrated force move transversely starting from position X1at girder G1 with level one of (10 kN) next to position X2 G2, position x3 at G3, finally on position x4 at G4, then after increasing the load to level two of (20 kN) and repeat the moving the applied loads,

finally increasing the load level to (30 kN) as shown in the Figure 6. Figure 7 and 8 show the point load application on the exterior and interior girders respectively.

Table 2: Dimension of tested bridge models

No.	Bridge Models	Central Span (m)	Radius (m)	Curvature (radian)	Girder Spacing (mm)
1	S200 C1	3.0	30	0.1	200
2	S200 C2	3.0	15	0.2	200
3	S200 C3	3.0	10	0.3	200
4	S175 C2	3.0	15	0.2	175
5	S175 C3	3.0	10	0.3	175

Table 3: Equivalent Loads

	Equivalent Self-weight(SW) (MPa)	Equivalent Superimposed dead load (SIDL) (MPa)
S175C2	0.096	0.0154
S175C3	0.096	0.0154
S200C1	0.093	0.0154
S200C2	0.093	0.0154
S200C3	0.093	0.0154

3. Numerical analysis

ANSYS WORKBENCH 14.5 commercial software [6] was used to perform the finite element analysis for curved I-girder bridge using solid modeling approach. The solid modeling used to reduce the required time for building the finite element model by direct generation.

1. Material modeling

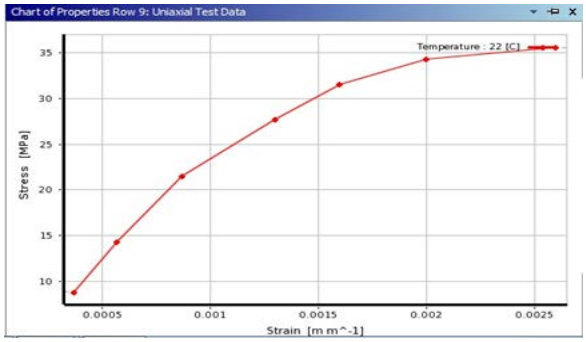

Figure 9: Concrete Material Modeling**.**

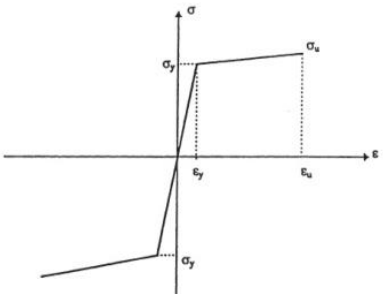

Figure 10: Idealized uniaxial stress-strain relationship for steel

The concrete modules of elasticity tests gives different results of stress-strain curve; the most appropriate experimental curve was selected to introduce the uniaxial stress-strain curve in the Finite Element model. Figure 9 shows the material concrete model was adopted in Finite Element analysis. Steel materials include, girders steel, stiffeners, diaphragms and steel reinforcements assumed to behave as an elastic-plastic model with strain hardening in both compression and tension [7]. Figure 10 shows stress-strain relationship was used to idealize the steel in the finite element analysis [8]. Table 4 shows the material properties used for finite element bridge model.

Table 4: Material properties used for finite element bridge model

Bridge Model Parte	Density (Kg/m^3)	Modulus of Elasticity (N/mm^2)	Poisson's Ratio	Tensile Yield Strength (MPa)	Tensile Ultimate Strength (MPa)	Ultimate Compressive Strength (MPa)
Concrete Deck	2100	25312	0.2	-	-	35.17
Steel Girders	7850	200000	0.3	374.61	525.33	--
Stiffeners & Diaphragms	7850	200000	0.3	355	454	--
Reinforcement Bar	7850	200000	0.3	650	815.6	--

2. Finite element modeling

ANSYS Worckbench 14.5 using a default element type Solid 185 for CAD geometry and Beam 188 for line bodies [6]. In this study Solis 185 was used to modeling all the steel parts (steel girders, stiffeners and diaphragms), Solid 65 to idealize the concrete deck and Link180 to idealize the double layer concrete deck

reinforcement. Solid185 is a default program selection for 3-D modeling of solid structure. It is defined by eight nodes having three translation degree of freedom in each nodal x, y and z direction. Figure 11a shows the Solid185 Homogeneous Structural Solid geometry which was used to idealize the bridge model steel parts. Solid65 Element is used for the three dimensional modeling of concrete deck slab with or without reinforcing bars (rebar) and defined by eight nodes having three degrees of freedom at each node: translations in the nodal x, y, and z directions. Figure 11b shows the Solid65 geometry which was used to idealize the concrete deck slab for the bridge model. Link180 is a 3-D spar, the element can be used to model trusses, sagging cables, links, springs and it is a uniaxial tension-compression element with three degrees of freedom, translations in the nodal x, y, and z directions per each node. Figure 11c shows the Link180 geometry. There are three techniques were used to idealize the steel reinforcement [5], as shown in Figure 12, (a) discrete model using a bar element connected with concrete mesh in the same nodes and the concrete mesh is restricted by the steel reinforcement location, also volume of the steel reinforcement is not deducted from the concrete volume, (b) embedded model because the stiffens of the reinforcing steel is evaluated separately from the concrete elements and this model built by the way keep the steel rebar displacement compatible with the surrounding concrete elements, (c) the smeared model assumes uniformly distribution of reinforcement throughout the concrete elements in a defined region of the FE mesh. The radial and tangential direction of the double layer steel reinforcement for the concrete deck of the curved I-girder bridge make the discrete approach difficult to use, since it is impossible to find the shared nodes between the steel reinforcement and concrete elements, therefor the embedded model be the best solution to idealize the steel reinforcement in the concrete deck slab for the bridge model.

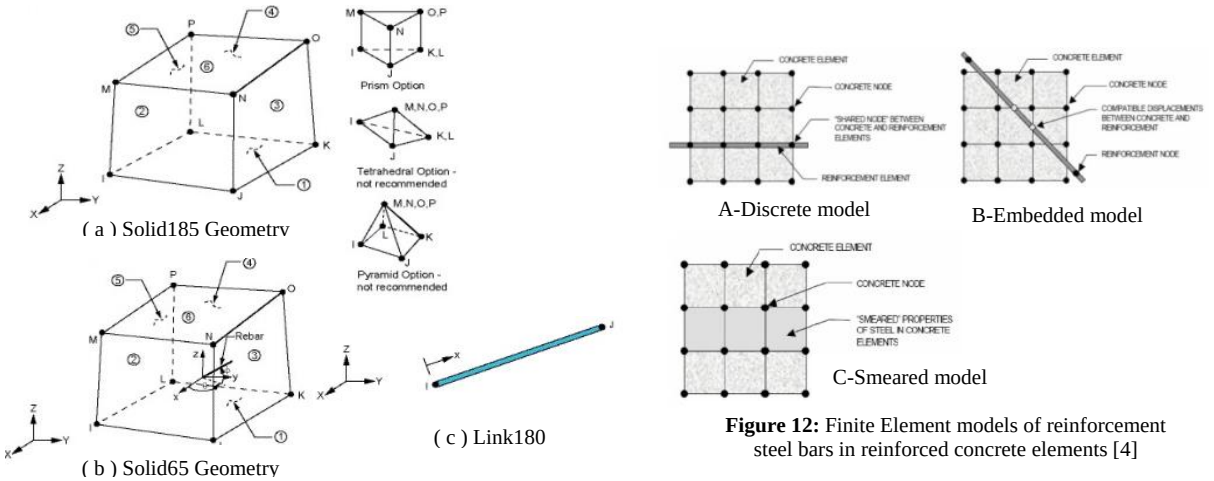

Figure 12: Finite Element models of reinforcement steel bars in reinforced concrete elements [4]

Figure 11: FE Geometry [3]

3. Meshing

ANSYS Worckbench 14.5 needs a primary element size to adopt it in the auto- mesh generation; the primary element size was selected as 15 mm, therefore there are two solid65 element through the concrete deck depth and there are 16 solid185 elements through the steel girder web depth, while there are a special mesh divisions for top and bottom steel girder flange due to flange width, curvature and the joint connection with transverse

diaphragms. The program auto-generation provides a triangular mesh for transvers diaphragms and a stiffener to overcome the girder-diaphragm problems, Figure 13 shows the mesh type, size and distribution for all the bridge model parts.

4. Loads

Self-weights, equivalents loads were applied on the curved I-girder bridge models, the loads of the bridge model was introduced by the ANSYS Worckbench 14.5 software as a uniform loads along the gravity direction, the equivalents self-weights and superimposed dead loads were applied as uniform distributed loads on the full concrete deck area in the gravity direction, the point load was applied as a concentrated load as shown in Figure 14.

5. Boundary conditions

ANSYS Worckbench 14.5[6] allows specifying supports along edges, faces and bodies. Hinge and roller supports was modeled along the bottom edges of each steel girders to perform the simply support behavior of the bridge model. Translation in global direction Y and Z were constrained as zero value and release the X translation in the left side support; while all translation were constrained as zero in the right support. Rotation was released around Y axis and prevented around the X and Z axis at each supports.

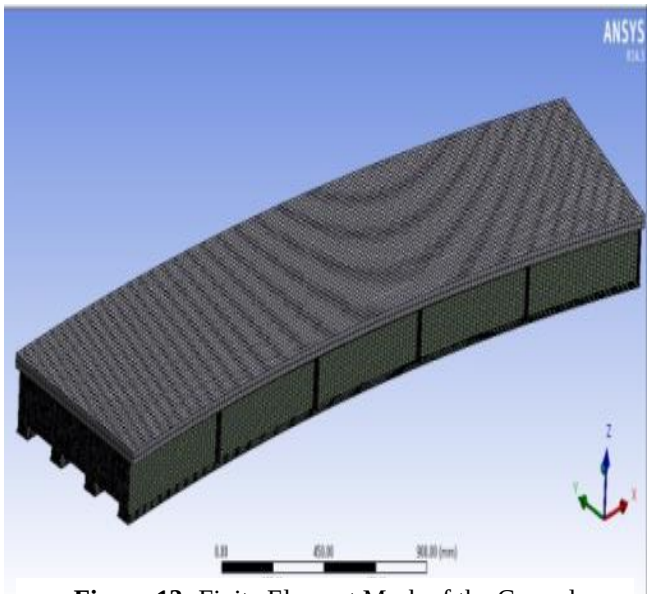

Figure 13: Finite Element Mesh of the Curved Bridge Model

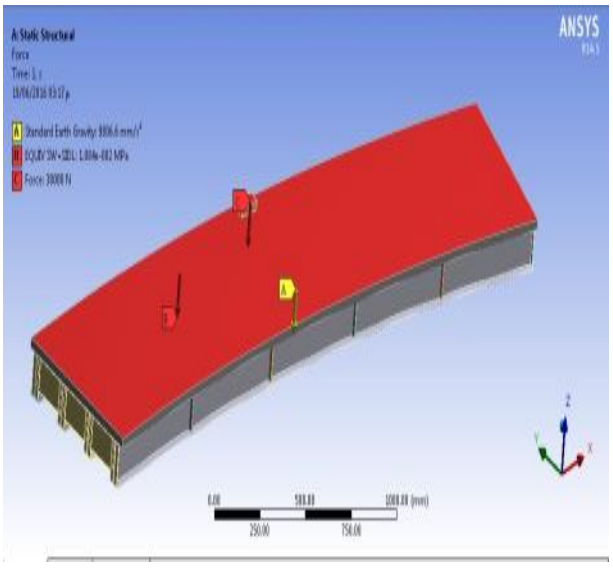

Figure 14: Finite Element-Load Application

4. Results and Discussions

4.1. Experimental results.

The experimental vertical load share results due to the point load at different locations X1, X2, X3 and X4 with

three levels 10, 20 and 30 kN were plotted for each loading case.

The calculation of girder vertical load share depends on the generated longitudinal stress at bottom flange of steel girder to the summation of these stresses for all girders in the bridge deck according to equation 1[8].

$$(GLS)_i = \frac{\sigma_i}{\sum_1^n \sigma_j} \qquad (1)$$

Where, GLS is the girder load share, σ_i and σ_j are the longitudinal stresses at bottom flange of the specified girders, these stresses were calculated due to only the effect of point load, and n is the number of the girders in the cross section.

The point load process was used as a simple practical approximate method to idealize the live load resultant. The used of three load level to study the variation of girders load share at multi-load levels. Figures 15 to 34 show the girders vertical load share due to point load for various position for all models specified in Table 2. For bridge model S175 C2, load level one (10 kN) give the maximum for G1, G2 and G4 as (0.552, 0.434, and 0.485 respectively), while the maximum GLS for G3 was 0.334 at second load level of 20 kN, that mean that the load share of each girder depend on the girder position and the magnitude of the applied load. For the bridge model S175 C3, the maximum GDF of G1 was (0.488) at level one (10 kN), the maximum GDF of G2, G3 and G4 was (0.380, 0.351 and 0.469) respectively at level three (30 kN), that is mean the increasing of the curvature make the girders G2,G3 and G4 takes the maximum loads under a point load in high load level. Increasing the girder spacing as well as decreasing the model curvature as for model S200 C1, in this bridge model the maximum GLS for all girders was at the first load level (10 kN) as shown in Figs 13 to 16.

The GLS of inner girder approximately has a similar with the outer girder under point load that because the smallest curvature ratio for this bridge model and the bridge behavior approximately approach to the behavior of straight bridge. For the bridge model S200 C2, The maximum GLS for G1 and G2 was 0.494 and 0.354 respectively at level one of 10 kN, while the maximum GDF of outer girders G3 and G4 was 0.325 and 0.471 at load level three (30 kN). In contrast with the bridge model S175 C2 , as girder spacing increased the maximum GDF of outer girder accord in third level of (30 kN), means that the curvature, girders spacing, load position and magnitude effect the girder vertical load share in the bridge deck.

The experimental results of the model S200 C3 show that the maximum GLS for G1 was 0.495 at level one of 10 kN, the maximum GLS of G2 was 0.372 at second load level (20 kN) and the maximum GDF of outer girders G3and G4 was 0.355 and 0.453 respectively at load level three (30 kN).

In the bridge model of S200 C2 the GLS of G2 was accorded in load level one (10 kN), while for bridge model S200 C3 it was accorded in load level two (20 kN), means that, as the bridge curvature increased , the maximum GLS of each girder under point load will accord in high load level. The effect of girder spacing appeared in value of GLS of the inner girder G2 comparing with bridge model S175 C3.

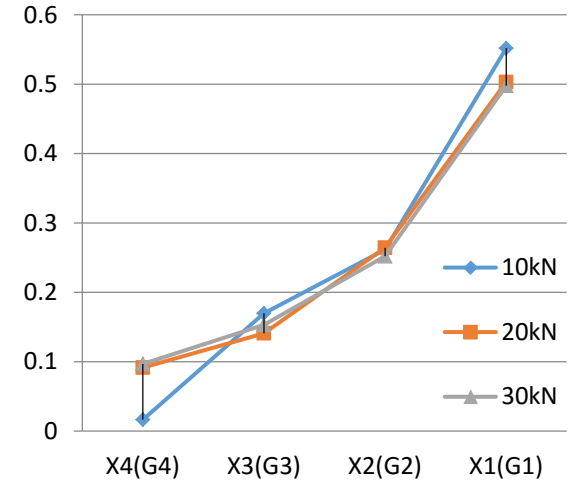

Figure 15: GLS-G1 (S175 C2)

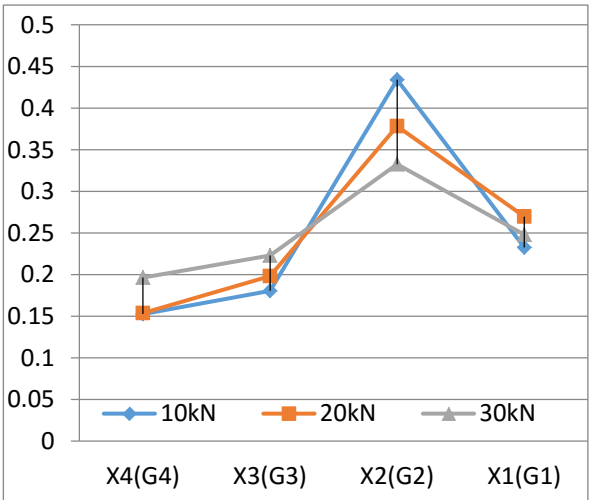

Figure 16: GLS-G2 (S175 C2)

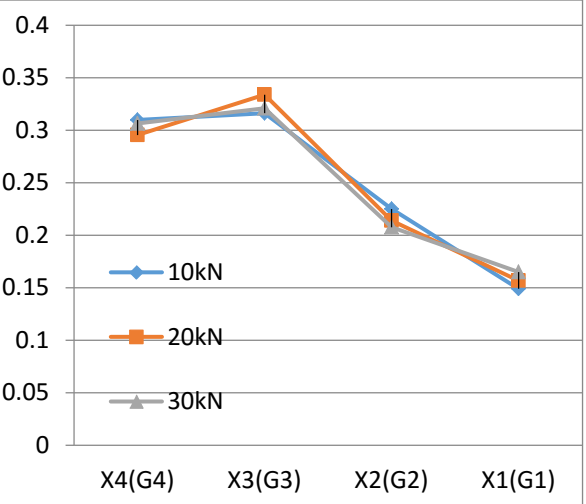

Figure 17: GLS-G3 (S175 C2)

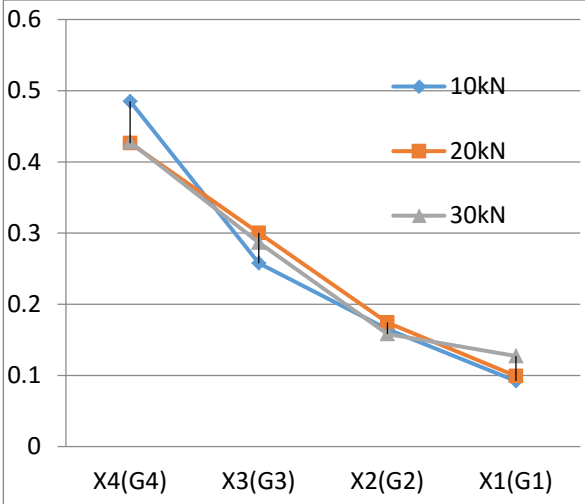

Figure 18: GLS-G4 (S175 C2)

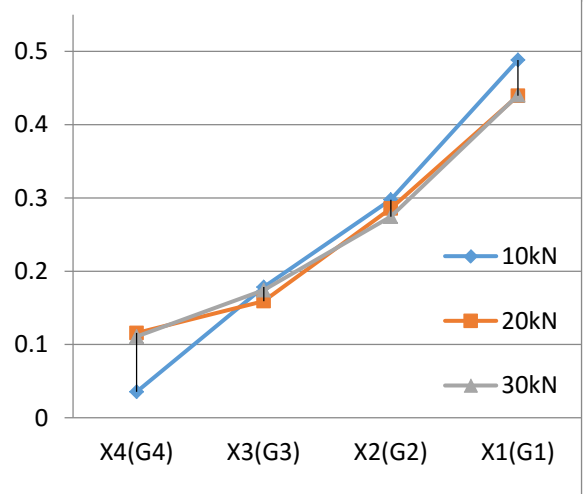

Figure 19: GLS- G1 (S175 C3)

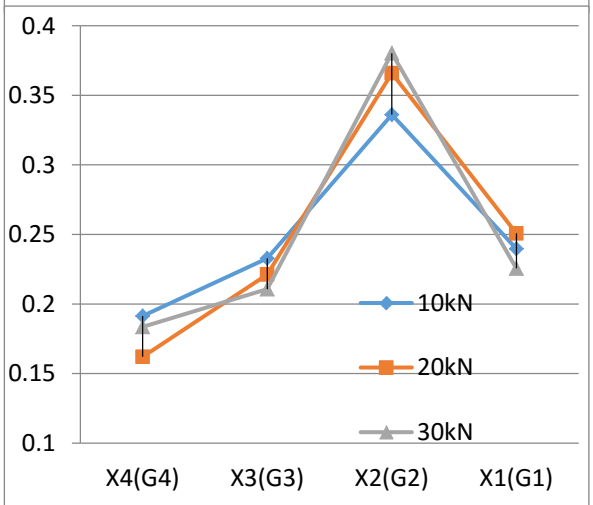

Figure 20: GLS- G2 (S175 C3)

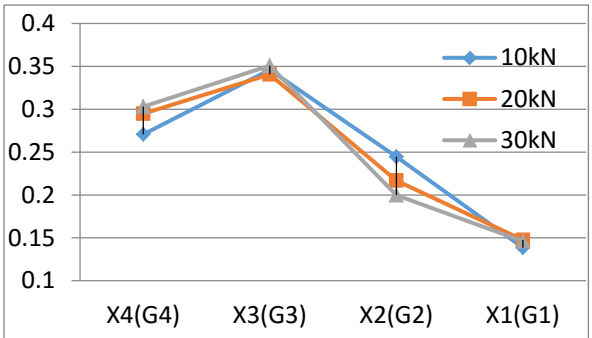

Figure 21: GLS- G3 (S175 C3)

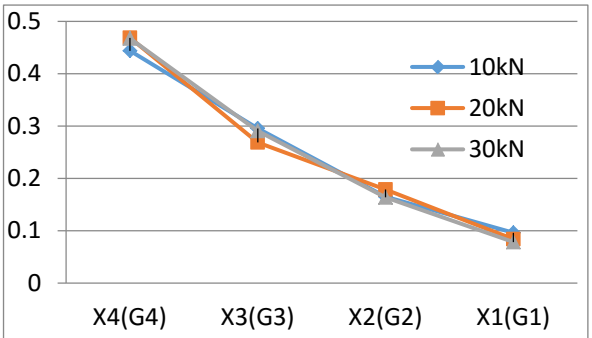

Figure 22: GLS- G4 (S175 C3)

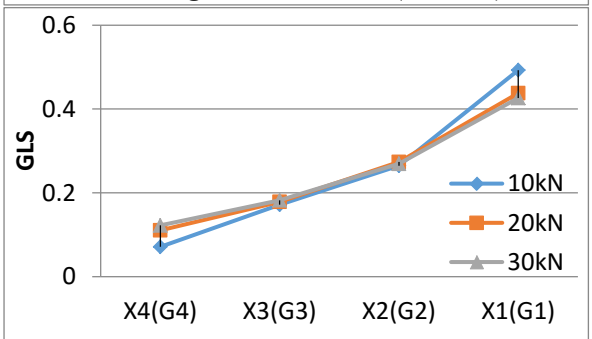

Figure 23: GLS-G1(S200 C1)

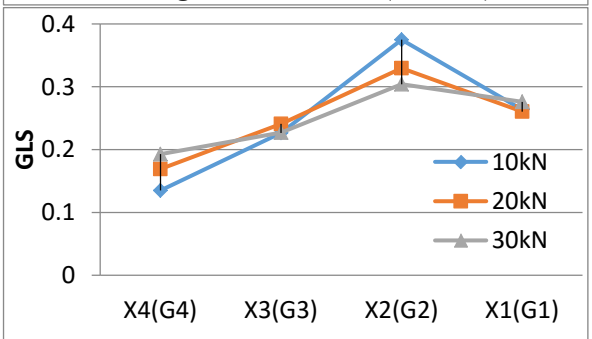

Figure 24: GLS-G2(S200 C1)

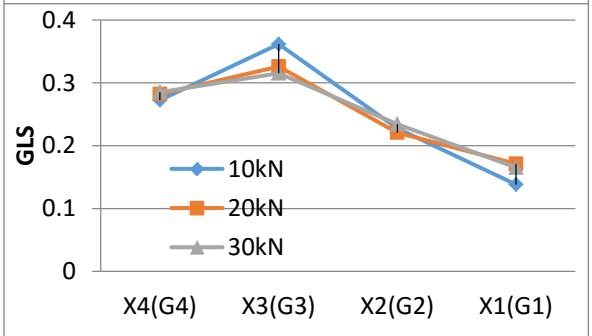

Figure 25: GLS-G3(S200 C1)

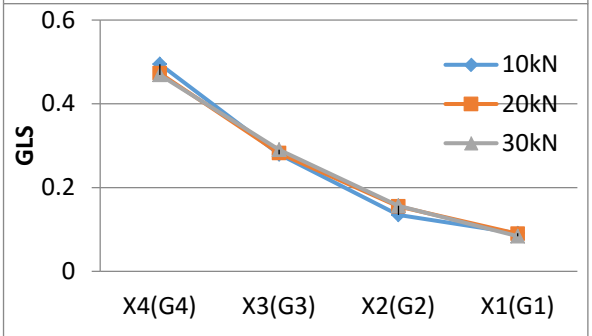

Figure 26: GLS-G4(S200 C1)

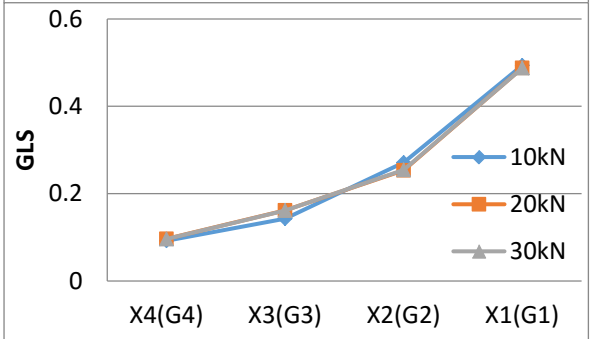

Figure 27: GLS-G1(S200 C2)

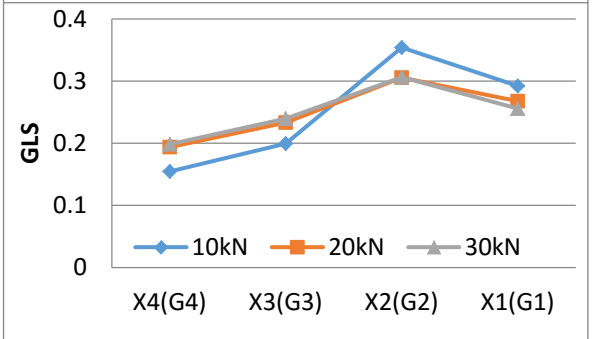

Figure 28: GLS-G2(S200 C2)

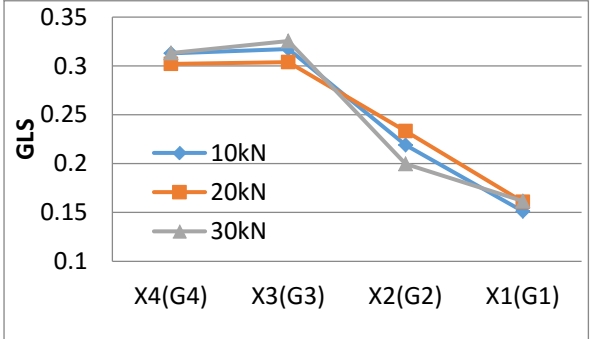

Figure 29: GLS-G3(S200 C2)

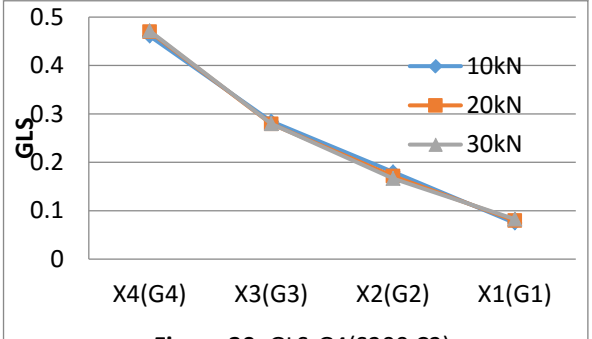

Figure 30: GLS-G4(S200 C2)

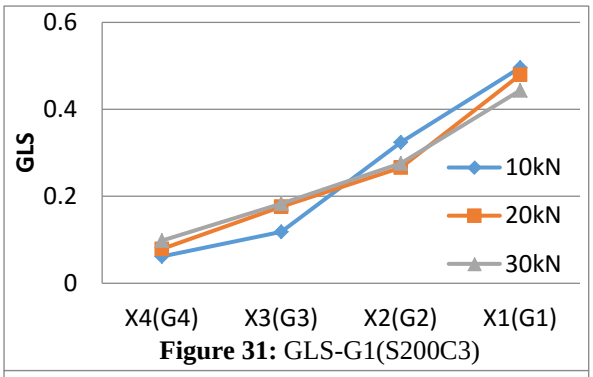

Figure 31: GLS-G1(S200C3)

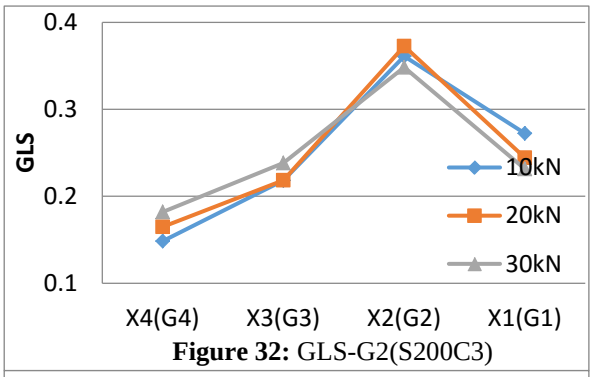

Figure 32: GLS-G2(S200C3)

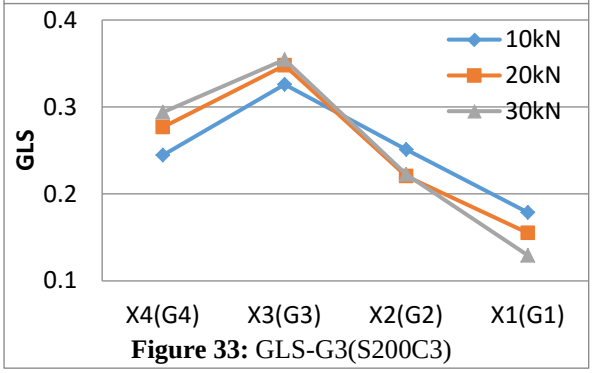

Figure 33: GLS-G3(S200C3)

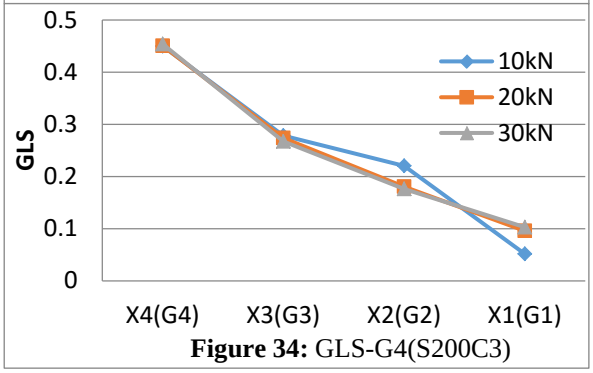

Figure 34: GLS-G4(S200C3)

4.2. Numerical results

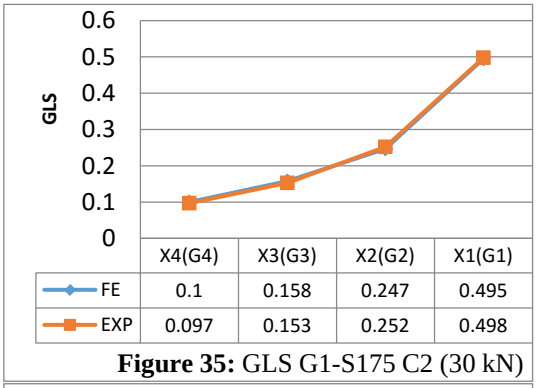

Figure 35: GLS G1-S175 C2 (30 kN)

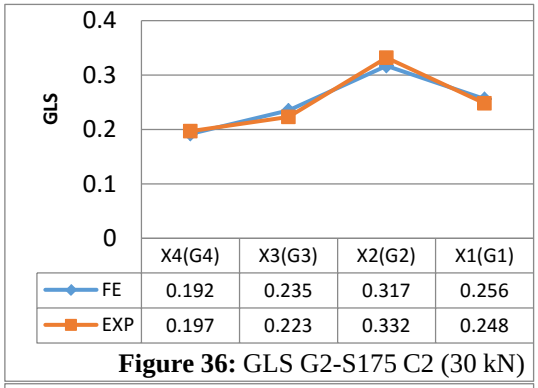

Figure 36: GLS G2-S175 C2 (30 kN)

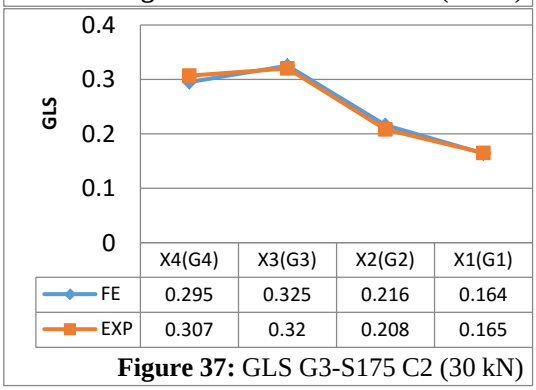

Figure 37: GLS G3-S175 C2 (30 kN)

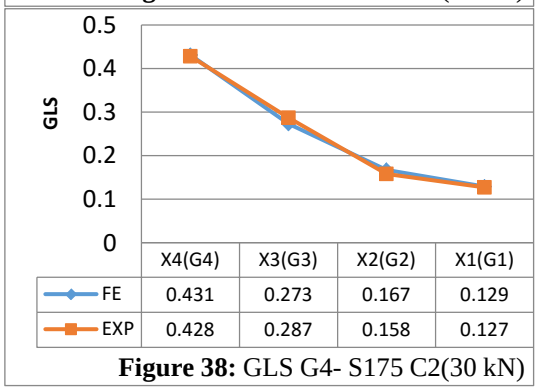

Figure 38: GLS G4- S175 C2(30 kN)

The comparison between the experimental and numerical results for the girders vertical load share (GLS) shows very good agreements, the maximum deviation in results reach to13% in such a single case, while the convergence results are the prevailing situation. Figs 35 to 54 show the comparison of GLS between the experimental and numerical results for load level of 30 kN for all tested models.

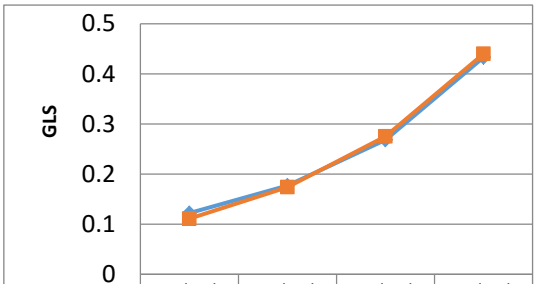

	X4(G4)	X3(G3)	X2(G2)	X1(G1)
FE	0.122	0.177	0.268	0.433
EXP	0.111	0.174	0.275	0.44

Figure 39: GLS G1- S175 C3 (30 kN)

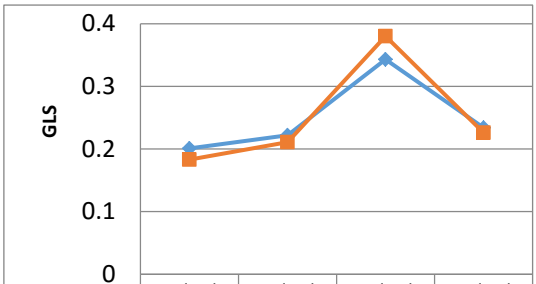

	X4(G4)	X3(G3)	X2(G2)	X1(G1)
FE	0.201	0.222	0.343	0.234
EXP	0.183	0.211	0.38	0.226

Figure 40: GLS G2- S175 C3 (30 kN)

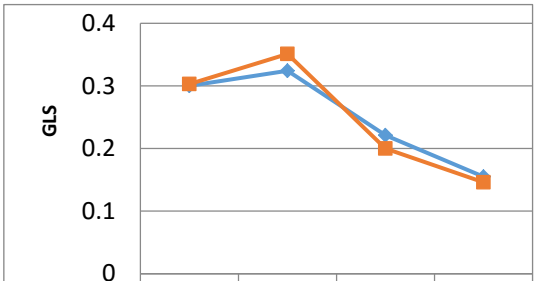

	X4(G4)	X3(G3)	X2(G2)	X1(G1)
FE	0.3	0.324	0.221	0.155
EXP	0.303	0.351	0.2	0.146

Figure 41: GLS G3- S175 C3 (30 kN)

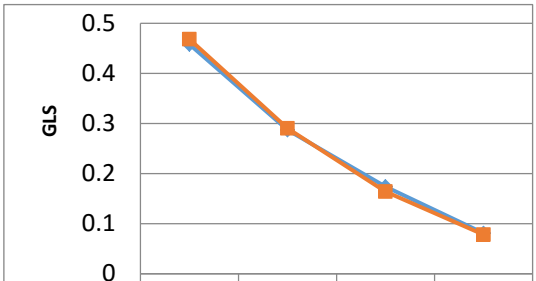

	X4(G4)	X3(G3)	X2(G2)	X1(G1)
FE	0.458	0.287	0.174	0.081
EXP	0.468	0.29	0.164	0.078

Figure 42: GLS G4- S175 C3 (30 kN)

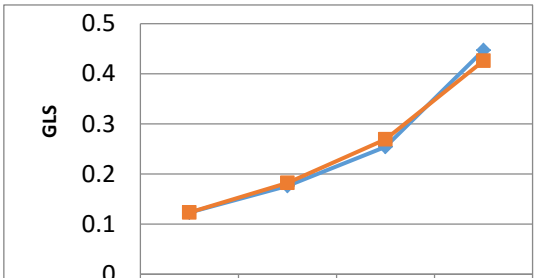

	X4(G4)	X3(G3)	X2(G2)	X1(G1)
FE	0.123	0.176	0.254	0.447
EXP	0.123	0.182	0.269	0.426

Figure 43: GLS G1- S200 C1 (30 kN)

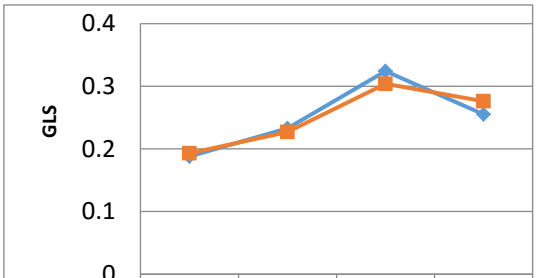

	X4(G4)	X3(G3)	X2(G2)	X1(G1)
FE	0.188	0.233	0.324	0.255
EXP	0.193	0.227	0.304	0.276

Figure 44: GLS G2- S200 C1 (30 kN)

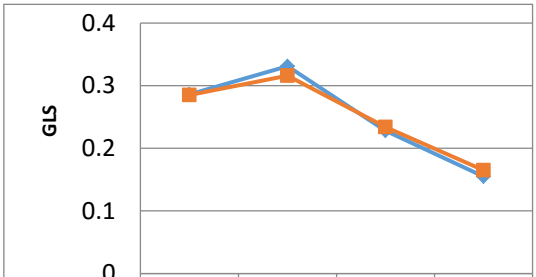

	X4(G4)	X3(G3)	X2(G2)	X1(G1)
FE	0.286	0.331	0.228	0.155
EXP	0.285	0.316	0.234	0.165

Figure 45: GLS G3- S200 C1 (30 kN)

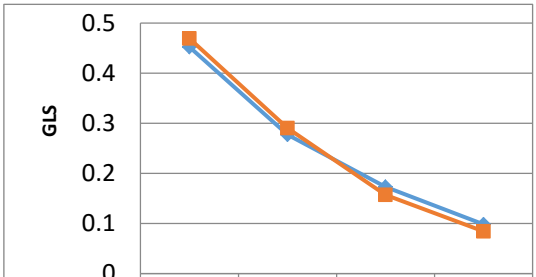

	X4(G4)	X3(G3)	X2(G2)	X1(G1)
FE	0.452	0.277	0.173	0.098
EXP	0.469	0.29	0.157	0.084

Figure 46: GLS G4- S200 C1 (30 kN)

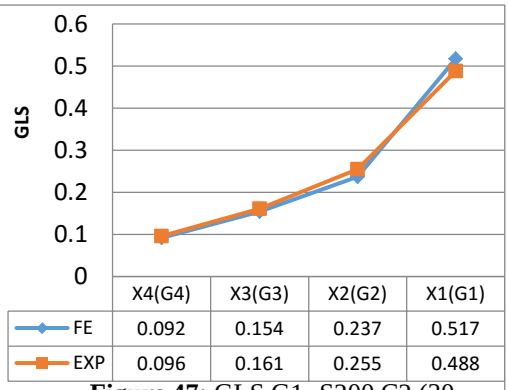

	X4(G4)	X3(G3)	X2(G2)	X1(G1)
FE	0.092	0.154	0.237	0.517
EXP	0.096	0.161	0.255	0.488

Figure 47: GLS G1- S200 C2 (30 kN)

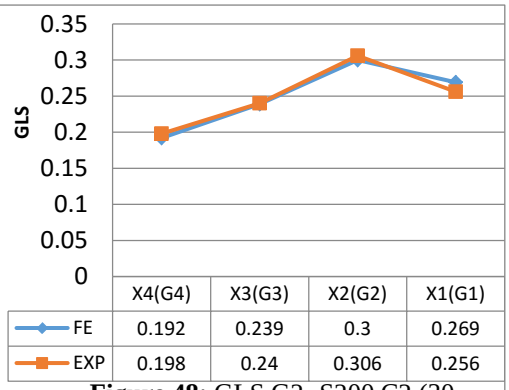

	X4(G4)	X3(G3)	X2(G2)	X1(G1)
FE	0.192	0.239	0.3	0.269
EXP	0.198	0.24	0.306	0.256

Figure 48: GLS G2- S200 C2 (30 kN)

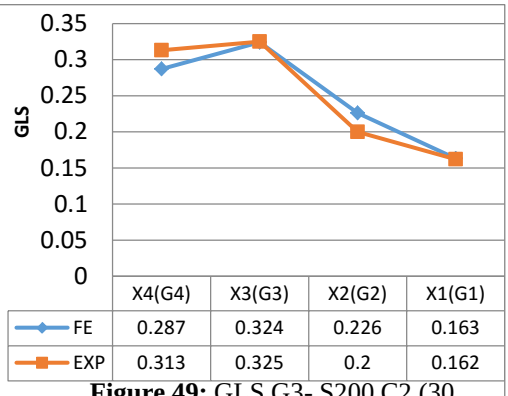

	X4(G4)	X3(G3)	X2(G2)	X1(G1)
FE	0.287	0.324	0.226	0.163
EXP	0.313	0.325	0.2	0.162

Figure 49: GLS G3- S200 C2 (30 kN)

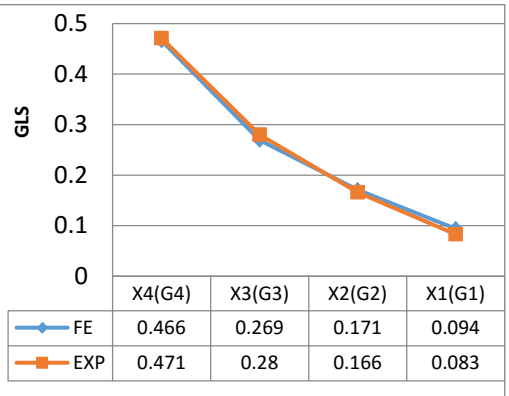

	X4(G4)	X3(G3)	X2(G2)	X1(G1)
FE	0.466	0.269	0.171	0.094
EXP	0.471	0.28	0.166	0.083

Figure 50: GLS G4- S200 C2 (30 kN)

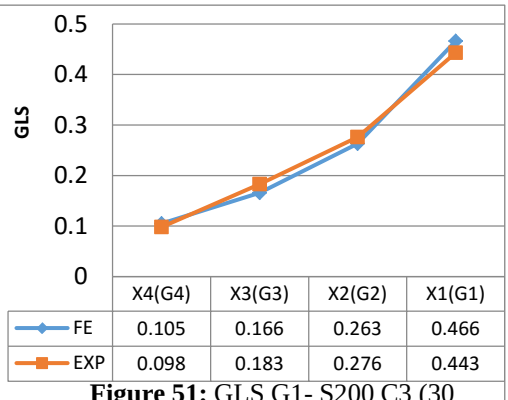

	X4(G4)	X3(G3)	X2(G2)	X1(G1)
FE	0.105	0.166	0.263	0.466
EXP	0.098	0.183	0.276	0.443

Figure 51: GLS G1- S200 C3 (30 kN)

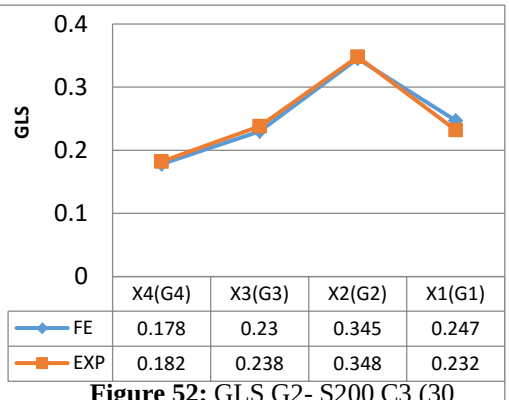

	X4(G4)	X3(G3)	X2(G2)	X1(G1)
FE	0.178	0.23	0.345	0.247
EXP	0.182	0.238	0.348	0.232

Figure 52: GLS G2- S200 C3 (30 kN)

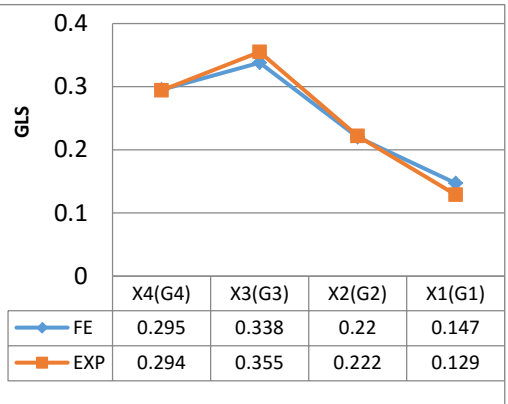

	X4(G4)	X3(G3)	X2(G2)	X1(G1)
FE	0.295	0.338	0.22	0.147
EXP	0.294	0.355	0.222	0.129

Figure 53: GLS G3- S200 C3 (30 kN)

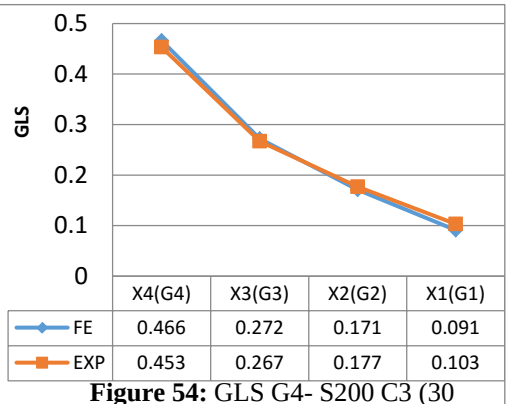

	X4(G4)	X3(G3)	X2(G2)	X1(G1)
FE	0.466	0.272	0.171	0.091
EXP	0.453	0.267	0.177	0.103

Figure 54: GLS G4- S200 C3 (30 kN)

5. Conclusions

The conclusions can be summarized as follow:

1. The main factors affecting the girder vertical load share were the point load position, load level and the bridge curvature value, while the girder spacing had a less effect.
2. The maximum GLS for the inner girder results when the point load was above this girder because the generated girder stresses is high relative to the total sectional stresses response that results from this loading case.
3. The maximum GLS for the inside girders (next to inner) depends on the curvature and the load level.
4. As the bridge curvature increased, the maximum GLS of each girder under point load will accord in high load level.
5. There are very good agreements between the experimental and numerical results, the maximum deviation in results reach to13% in such a single case, while the convergence results are the prevailing situation.

6. Recommendations

Research program may be extended to study the:

1. Ultimate load capacity of the horizontally curved in plane composite concrete-steel I-girder bridges.
2. Impact response of horizontally curved in plane composite concrete-steel I-girder bridges.

References

[1]. American Association of State Highway and Transportation Officials, AASHTO. 2012. Standard Specifications for Highway Bridges. Washington, D.C AASHTO LRFD Bridge Design Specification, Sixth edition, 2012.

[2]. A. Zuerick, and R. Naqib, "Horizontally Curved Steel I-Girders State-of-the-Art Analysis Methods", Journal of Bridge Engineering, 4 (1): 38-47, 1999.

[3]. American Association for State Highway and Transportation Officials, AASHTO. 1993. Specification for Horizontally Curved Highway Bridges. Washington, D.C.

[4]. T. Stegmann and T. V. Galambos, (1976). "Load factor design criteria for curved steel girders of open cross section." Washington Univ. Research Rep. No. 43, Washington Univ., St. Louis.

[5]. V. Thevendran et. al. "Experimental study on steel-concrete composite beams curved in plan" Engineering Structures 22 (2000) 877–889.

[6]. Ansys Workbench 14.5 help,2012

[7]. F. A. Tavarez, "Simulation of Behaviour of Composite Grid Reinforced Concrete Beams Using Explicit Finite Element Method", M. Sc. Thesis, University of Wisconsin-Madison, Wisconsin, 2001.

[8]. Jerad J. Hoffman "Analytical and field investigation of horizontally curved girder bridges ". M.A.SC. Thesis submitted in Civil Engineering Dept., Iowa State University 2013.